Post Access Report

Extreme events modelling for the MARMOK-OWC wave energy converter

Awardee: IDOM Inc.

Awardee point of contact: Borja de Miguel Para

Facility: Sandia National Laboratories (Sandia)

Facility point of contact: Chris Chartrand

Technical Point of Contact: Jessica Nguyen

Date: 08/02/2024

TEAMER
Testing & Expertise for Marine Energy

EXECUTIVE SUMMARY

Through the TEAMER program, Sandia National Laboratories (SNL) collaborated with IDOM Incorporated to study their MARMOK-OWC wave energy conversion device. The study yielded a quantitative understanding of hydrodynamic pressures on the oscillating water column (OWC) device surfaces, the mooring tensions, and the dynamic performance of the device under extreme ocean wave conditions. This project will utilize a comprehensive multi-phase Navier-Stokes flow solver with an overset body-fit mesh to predict fluid velocities and hydrodynamic forces on the MARMOK OWC device. Computational Fluid Dynamics (CFD) analysis will be conducted using OpenFOAM

In Task 1, three different extreme sea state time series were successfully recreated in numerical simulations using wave elevations provided by IDOM from previous tank test data. In Task 2, the MARMOK-OWC system was simulated under two of these irregular sea states (the two steepest ones; one sea state was not simulated due to time constraints). During the simulations, the MARMOK-OWC system was kept fixed while wave pressures and the loadings on the hull structure were recorded. These data were extracted and provided to IDOM for further study of structural loadings. Task 3 included numerical simulations of free-decay tests, which showed good comparisons with experimental data. In Task 4, we successfully integrated OpenFOAM and MoorDyn to realistically model the physical mooring system, consisting of chains, polyester ropes, and connecting surface buoys. We also conducted four fully coupled simulations for two different hull scales and two mooring configurations. While three simulations were completed successfully, one simulation resulted in instability when the device was subjected to the highest nonlinear wave signal. Due to project time constraints, further investigation was not feasible, but this issue will be of interest for future study and funding.

Overall, these results significantly enhanced the knowledge at IDOM and national labs regarding the behavior of such devices under extreme sea conditions and the complexities of numerical modeling in highly nonlinear environments. This knowledge will be pivotal in streamlining device modeling, design processes, and advancing the efficiency and effectiveness of clean energy device development in the future.

1 INTRODUCTION TO THE PROJECT

The MARMOK-OWC wave energy converter is a spar type oscillating water column, with no moving parts except the air turbine itself, and all the critical elements (Power Take-Off (PTO) included) are not exposed directly to waves. A picture of the most recent offshore deployment of a low power prototype can be found in Figure 1.

Figure 1: Individual MAMOK-OWC deployment

Extreme loads are one of the main inputs in the Wave Energy Converter (WEC) structural and mooring systems design, which determine the system cost for each deployment location. The cost of these two subsystems are the largest of the capital expenditure (CAPEX) of the technology so they have a significant impact on the system levelized cost of energy (LCOE). Currently, these extreme loads are based on conservative approaches suggested by standards which require validation through laboratory testing. A better understanding of these loads, and having a flexible numerical model to estimate loads, can potentially lead to a structural and mooring design refinement which will reduce system cost with a significant impact on LCOE.

The project will utilize high fidelity simulation to quantify forces and moments on the spar buoy and the tension forces on the mooring lines used for station keeping, which result from by incident waves during typical and extreme events.

Model validation will be performed with laboratory tests results of the testing campaign recently executed under FOA 2080, to give confidence to the forces and tensions predicted by simulation.

2 ROLES AND RESPONSIBILITIES OF PROJECT PARTICIPANTS

2.1 APPLICANT RESPONSIBILITIES AND TASKS PERFORMED

- Borja de Miguel Para
  - Project Management
- Jon Morgaetxeberria
  - Support on results analysis for structural and mooring design

2.2 Network Facility Responsibilities and Tasks Performed

- Chris Chartrand
  - Project management
  - Simulation performance and analysis
- Jessica Nguyen
  - Mooring expert
  - Simulation model setup, performance, and analysis

3 Project Objectives

The technical assistance objectives are to conduct computer-based modelling and analysis of a fully coupled, multi-phase fluid, transitive, high fidelity simulation of the spar OWC device under wave excitation, utilizing Volume-of-Fluids (VOF) representation, 6DOF motion models, and linear spring mooring force representation. This will be performed using OpenFOAM on Sandia's high performance computing resources.

The specific tasks requested are:

1) Simulation of Irregular waves using a spectrum representative of the operational environment (previous studies under FOA 2080 were limited to regular wave conditions).
2) Simulation of a static MARMOK-OWC under hydrodynamic loads from the representative irregular waves.
3) Free decay testing of the floating MARMOK-OWC under buoyancy and mooring forces. This test will validate the mooring force model and identify any adjustments which need to be made before the final simulation.
4) Full 6DOF simulation of the MARMOK-OWC subject to hydrodynamic forces, and mooring forces in the operational area's representative irregular waves

4 Test Facility, Equipment, Software, and Technical Expertise

All analysis will be performed on Sandia computers and clusters, using OpenFOAM software. Sandia technical staff trained in CFD simulation will provide the labor and analysis for this project.

5 Test or Analysis Article Description

The basic device concept of the OWC can be described as a spar element holding a cylindrical water column in the interior. These two bodies, the device structure and the internal water column, are coupled by the PTO and are designed to be excited by the incoming waves, each with different resonance periods, so that relative movement between the two bodies is enhanced. An air chamber is kept confined in the upper side of the water column, whose compression and decompression is forced to pass through a self-rectifying air turbine. This working principle can be illustrated in the following figure (Figure 2):

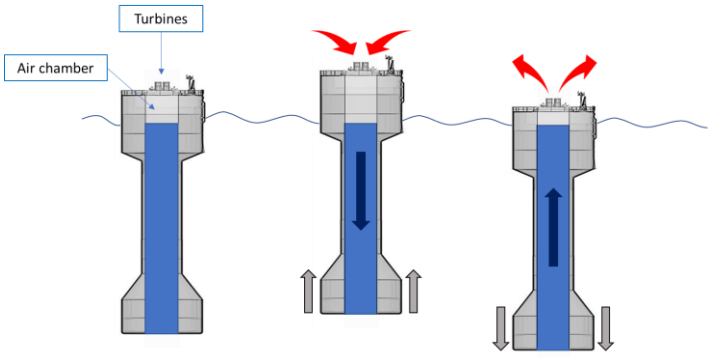

Figure 2: Illustration of the MARMOK oscillating water column device concept and the air turbine PTO.

Regarding the mooring system, it is composed of a submerged cell, kept in position by 4 catenary lines, and 4 additional diagonal lines per unit connecting it to the cell. This configuration, dubbed "KARRATU" relieves the device of the need to withstand the weight of the catenary lines, while allows minimal interference with the active degree of freedom, that is, heave motion.

The shared mooring configuration further facilitates multi-unit device deployments achieving a significant reduction in costs. Besides, it provides a better utilization of the sea surface (i.e. higher density) compared to individually moored WECs. This mooring configuration is already used in aquaculture. See Figure 3. It is noted that while the shared mooring configuration is desired as the development expands to multi-WECs, the current study focuses on the single WEC performance only.

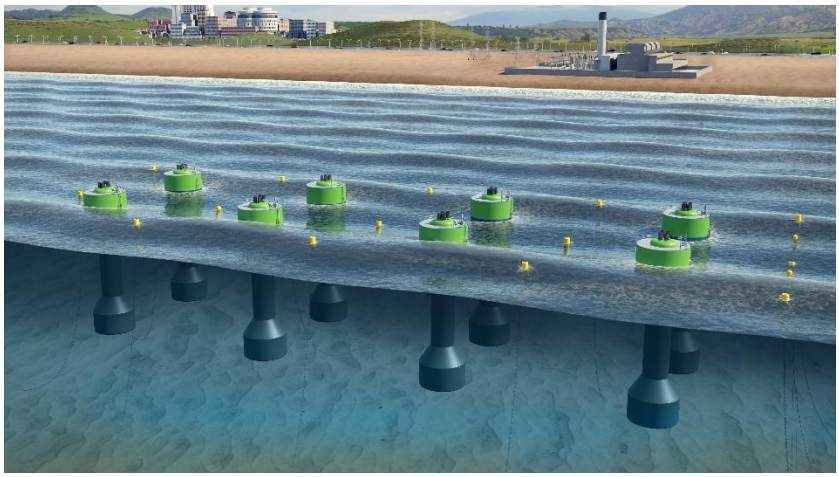

Figure 3: MARMOK-OWC array deployment

When analyzing the cost breakdown of most of wave energy converters, main cost contribution come from the structure and mooring system cost. Consequently, in order to achieve a competitive long term LCOE, these systems designs have to be optimized. The first step for this optimization is obtaining a flexible and reliable numerical tool to estimate extreme loads in both structure and mooring system which can be used during design phase before reaching the laboratory testing phase, where the introduction of design modifications is more difficult and costly.

The development of a procedure for the detailed analysis of such a critical aspect of the design of any wave energy converter, like extreme events are, will boost the development process of the technology, enabling the optimization of the structural design, station keeping system and PTO essentially, resulting in a competitive cost-effective device design.

6 WORK PLAN

6.1 NUMERICAL MODEL DESCRIPTION

This project will utilize a comprehensive multi-phase Navier-Stokes flow solver with an overset body-fit mesh to predict fluid velocities and hydrodynamic forces on the MARMOK OWC device. Surface pressures on the device, mooring tensions, wave elevations, along with system's motions will be recorded and converted into external forces for analysis by IDOM. To accurately represent the device's kinematics under wave conditions, a realistic mooring line model will be employed instead of a simplified spring-damper model.

CFD analysis will be conducted using OpenFOAM, a validated, verified, and widely used open-source computational fluid dynamics package. OpenFOAM is freely available, enabling the transfer of all input files and configurations to the awardee for future studies beyond the TEAMER project. It supports various dynamic mesh methods, including recent versions (starting with v1706) that feature overset mesh functionality. This capability is essential for simulating complex geometries interacting with nonlinear wave conditions, such as high and steep waves, while maintaining high-quality meshing around both the solid body and the wave surface. OpenFOAM's built-in wave generation and absorption mechanisms will also be utilized.

The mooring system will be modelled using MoorDyn, an open-source lumped-mass model designed to simulate the dynamics of mooring systems connected to floating offshore structures. MoorDyn accounts for internal axial stiffness and damping forces, weight and buoyancy forces, hydrodynamic forces using Morison's equation (for calm water conditions), and vertical spring-damper forces from seabed contact. It also supports mooring lines with multiple segments of varying materials and the addition of clump weights or floats. Its open-source framework allows for modifications to incorporate highly nonlinear material properties if necessary.

Task 1: Numerical simulation of irregular sea states

Discussion: Baseline simulations will be performed modeling the sea states of interest. These simulations will iron out any issues relating to computational grid discretization, numerical schemes, and volume of fluids representation. Sandia will work with IDOM to select appropriate flow conditions sufficient for designing against extreme events (loads). Sandia will build and run the models and return the results of the simulations to IDOM for discussion.

Deliverable: Sandia will perform baseline simulations of 3 seas states prescribed by IDOM. Results will be delivered in the form of water surface heights as a function of time a position. Spectral analysis will be performed to confirm sea states are being accurately represented. All conclusions about inflow

conditions, grid discretization and solution methods will be documented and used to inform subsequent device simulations.

Task 2: Simulation of the fixed device under wave conditions

Discussion: An overset simulation will be set up with a body fit mesh around the MARMOK device and a regular grid covering the wave background. This simulation will couple the VOF wave model to the device representation, outputting pressure contours on the body surface. Any numerical complications resulting from the use of the overset model will be ironed out here. Sandia will build and run all models and return the results of the simulations to IDOM for verification and discussion.

Deliverable: Simulations will be performed on the device geometry and pressure contours, and integrated forces will be calculated and reported. Structural load quantities will be reported and any conclusions drawn from these results will be shared with IDOM.

Task 3: Free decay testing of the device

Discussion: This task will characterize the effects of the mooring lines and validate the spring force model used to represent them. The goal is to determine accurate representation of all external body forces before commencing the large, computationally expensive production runs. Sandia will work with IDOM to accurately model mooring line forces as seen by the full-scale device. Sandia will build and run the models and return the results of the simulations to IDOM for discussion.

Deliverable: In task 3, the effects of mooring lines be quantified, and mooring models will be validated. The MARMOK device will be raised above the equilibrium balance point and allowed to undergo free decay oscillations. The total force on the WEC device moorings will be calculated and reported as a function of time and device displacement for validation against data.

Task 4: Fully coupled simulation of wave driven device motion

Discussion: The previous tasks simulate the MARMOK under wave conditions and mooring line forces to isolate the respective effects. This task will couple the effects of irregular waves and mooring line station keeping in a single robust simulation. Sandia will work with IDOM to select the wave conditions to be explored. Sandia will build and run the models and return the results of the simulations to IDOM for discussion. It is anticipated that at least 2 fully coupled, 3D simulations will be run, but more will be explored should time allow.

Deliverable: Similar to task 3, the hydrodynamic effects will be quantified, this time with full rigid body dynamic coupling. The total hydrodynamic force on the WEC device will be calculated and the induced device accelerations will be simulated. Global forces on the WEC structure will be calculated by post-processing the pressure contours around the body surface. This information will be communicated to IDOM in the form of a performance table.

Task 5: Data compilation and analysis

Discussion: During the simulation performance data will continually be disseminated to IDOM for analysis and comparison to data. This will be used to guide the simulation process and validate results. Likewise, predictive simulations will be performed and used to guide device design.

Deliverable: All simulation data will be delivered to IDOM. IDOMs analysis and conclusions will be derived to Sandia. IDOM will compose a journal submission and Sandia will compile the final TEAMER reports and any potential conference/journal papers.

6.2 Test and Analysis Matrix and Schedule

The numerical tests performed consist of:

1) Month 1
    a. Demonstration of solver methodology, boundary condition implementation, closure equations, wall and symmetry assumptions, and output metrics on a sea states provided by IDOM.
    b. Verify that all required output is being produced in the format and frequency which is of best utility to the developer.
    c. Grid study. Choose discretization which provides adequate results convergence and agreement with available data as determined by IDOM.
2) Month 2-3
    a. Fixed buoy pressure analysis.
    b. Using ocean simulation from month 1, fluid-structure interaction and hydrodynamic forces will be calculated and shared with IDOM for validation.
3) Months 4-5
    a. Free decay simulation.
    b. Under static water conditions, and tensioned mooring forces, the MARMOK device will be lifted above its equilibrium balance point and allowed to decay naturally.
    c. Results will be compared to IDOM tank data for verification.
4) Months 5-23
    a. Fully coupled 3D simulation of the MARMOK device under gravitational, buoyant, and mooring line forces
    b. Simulations and analysis, quantifying pressure loads due to hydrodynamic and mooring line forces under extreme events.

Month #	1	2	3	4	5	6	7	8	9	10	11	12	13	14	15	16	17	18	19	20	21	22	23
Tasks																							
Task 1: Irregular waves modelling																							
Task 2: Static buoy modelling																							
Task 3: Free decay tests																							
Task 4: Full 6DoF modelling																							
Task 5: Analysis and Reporting																							

Milestones	Description
M1	Numerical model prepared to simulate irregular sea states (No buoy)
M2	Inclusion of the fixed buoy into the model
M3	Free decay tests performed and compared with tank testing resutls
M4	Fully coupled VOF, 6DoF, and mooring model simulations
M5	Data compilation and analysis, Final report submission sumarizing the work performed, Journal submission

6.3 SAFETY

There are no safety risks associated with this project.

6.4 CONTINGENCY PLANS

In the event that simulations need to be run longer than anticipated, either for better statistical representation of due to more detailed grid resolution being required, it may be necessary to concentrate efforts on fewer, more thoroughly analyzed, studies.

6.5 DATA MANAGEMENT, PROCESSING, AND ANALYSIS

6.5.1 Data Management

Data will be generated on Sandia's computing clusters. Analysis and post processed data will be stored on Sandia's data storage systems and shared with IDOM. All configuration files, input conditions, final reports and presentations will be retained by Sandia and shared with IDOM.

6.5.2 Data Processing

Data from early simulation time will be analyzed before the entire computation is completed. Preliminary results will be reviewed and compared to expected data as provided by IDOM. Anomalies will be investigated further and used to diagnose any simulation issues early in the process.

6.5.3 Data Analysis

Data will be collected natively by the simulation software. Most quantities of interest will be identified by IDOM prior to simulation work taking place, however upon investigation of the results during early stage simulation additional quantities may be identified to be of interest and modifications will be made accordingly.

7 PROJECT OUTCOMES

7.1. RESULTS

7.1.1 Task 1 – Numerical simulations of irregular waves

Three irregular wave conditions (TABLE 1) were selected for the simulations in this task. These were extracted from the full laboratory testing campaign performed where the sea states were selected from the PACWAVE-South occurrence matrix and 100yr environmental contour. So a moderate sea state, an energetic sea state and an survival sea state were selected for this task. The 3D numerical wave tank (NWT) is first constructed with parameterized dimensions of 4.0 wave length (see TABLE 1), λ, in the wave propagation direction and 0.5λ in the transverse direction. The wavelength is calculated by solving the dispersion equation as shown in equation (1). Newton-Raphson method was employed to solve the implicit equation iteratively with the error tolerance set at 1E-8. The water depth is modelled to match the experimental setup, with a depth (h) of 5.8 m. The still water level is set at 0 m, and several wave probes are placed along the tank such that they represent the experimental setup for consistent comparison. It is noted that due to the different in lengths of the NWT and the physical tank, the WEC location will be used as the reference point, and other probes will be placed with respect to this. Specifically, one probe is placed at 0.714 m upstream of the float's position. This probe is most essential

TABLE 1
IRREGULAR WAVE CONDITIONS

Test Name	E503	D516	H601
$H_s(m)$	2.25	4.75	7.39
$T_p(s)$	9.81	12.12	11.42
$\lambda\ (m)$	5.366	8.189	7.272

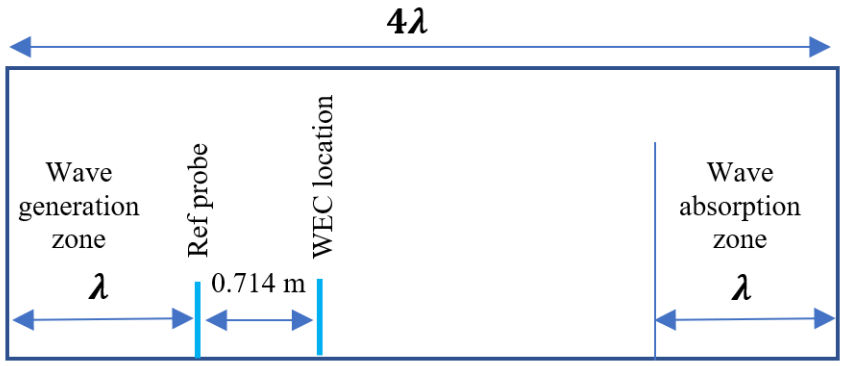

Figure 4: Numerical wave tank schematic. The relaxation zones for wave generation and absorption are one wave length, λ. The reference probe is placed at 0.714 m upstream of the WEC's location to be consistent with the experimental setup.

since it is used for the benchmark of the generated wave heights. One probe is placed at the WEC location, and two other wave probes (not shown in the figure) are placed downstream of the WEC body at a distance of 0.563m and 1.126m, respectively. A schematic of the tank setup is illustrated in Figure 4.

To replicate the time series of the experimental wave heights, the irregular wave signal is transformed using Fast Fourier Transformation (FFT) into a combination of sinusoidal waves. The wave components including amplitudes, frequencies, and phases taken from the FFT serve as input for the numerical wave maker. A phase shift is also implemented in the wave component input to represent the non-zero location of the reference probe in the experiment. In the waves2Foam library, this input of wave components is facilitated using the 'irregular' wave options. For the signal decomposition, a total of 300 frequencies are employed to capture the characteristics of the wave signal.

$$\lambda = \frac{g}{2\pi} T_p^2 \tanh\left(2\pi \frac{h}{\lambda}\right) \tag{1}$$

A mesh convergence study is also performed employing different grid sizes from 10-30 cells per wave height. It is noted that for overset technique, the horizontal and vertical grid sizes should be comparable at least in the region near the interpolation points. This ensures that when the meshes overlaps, the interpolation from one region to another stays consistent. Due to the length of the signal, it is not practical to compare individual components of the wave surface to determine convergence. We employ the significant wave height, which is computed from the signal spectral moment, as the convergence parameter.

The significant wave heights were estimated using the generated signal, from which the spectral density can be derived along with the zeroth spectral moment (Holthuijsen, 2010) as

$$H_s = 4\sqrt{m_o} \tag{3}$$

These values were then compared to the desired H_s, which was derived from the experimental value, and they are also employed to gage the convergence of the generated waves using different grid sizes**.** The scaled results (scale ratio is 1:15 for consistency with the tank test data) for three wave conditions are presented in Figure 5 to Figure 7. The simulated H_s suggested that the E503 and H601 cases converge rather quickly with the differences (within 1%) between the mesh resolutions are small and insignificant.

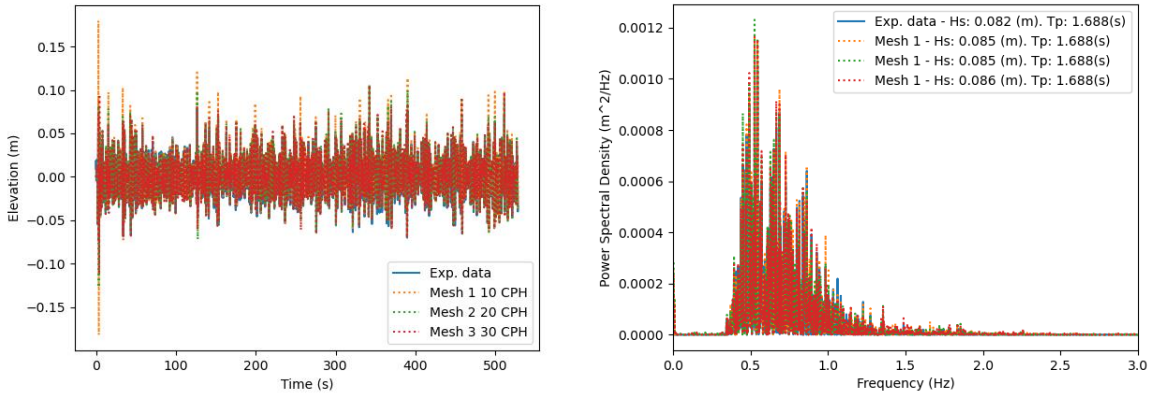

Figure 5: E503 case. Left: Time series of the generated wave. Right: Spectral density plot. The significant wave heights computed for different mesh sizes are also included. The differences with the input signal and the variations between the grid sizes are small indicating the convergence of the mesh at the lowest grid size of 10 cells per height.

The case is noted to converge at around 10 cells per wave height (CPH). The D516 case, on the other hand, is observed to achieve similar converged results with 20 cells per wave height.

The peak period, T_p, which was determined at the frequency with the highest spectral density, was also compared between the experimental data and different mesh resolutions. In general, T_p values compared very well across all the datasets. Their values are included in Figure 5-Figure 7.

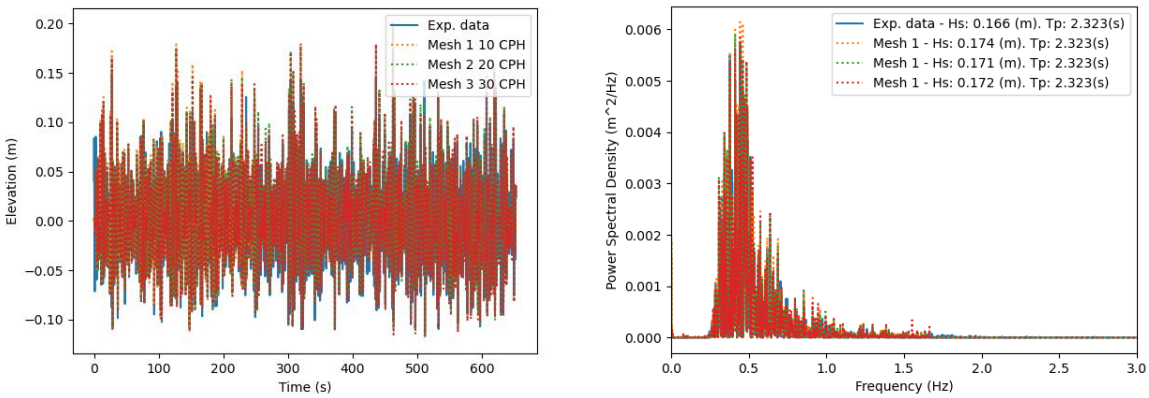

Figure 6: D516 case. Left: Time series of the generated wave. Right: Spectral density plot the differences with the input signal and the variations between the grid sizes are small indicating the convergence of the mesh at the lowest grid size of 20 cells per height.

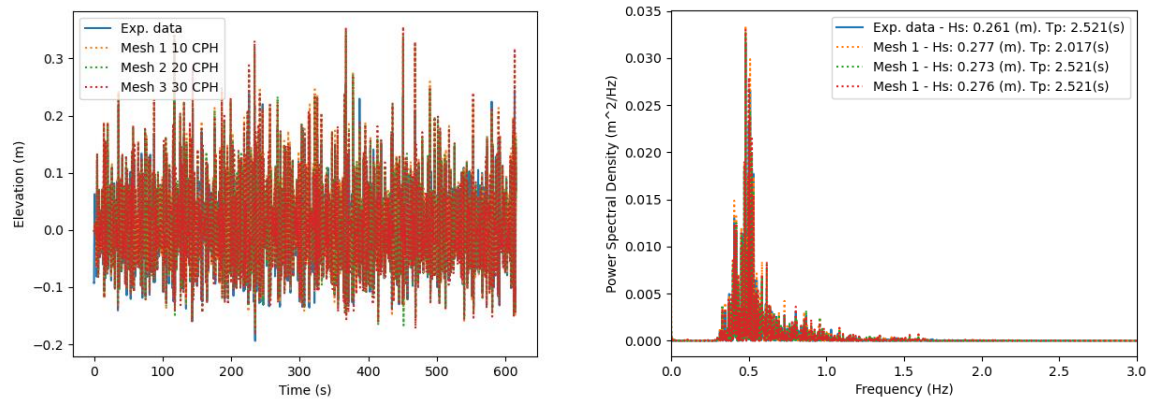

Figure 7: H601 case. Left: Time series of the generated wave. Right: Spectral density plot. The significant wave heights computed for different mesh sizes are also included. The differences with the input signal and the variations between the grid sizes are small indicating the convergence of the mesh at the lowest grid size of 20 cells per height.

7.1.2 Overset and background mesh construction for Tasks 2 – 4

Employing the results from the previous section, the overset mesh, which combines the body-fitted mesh and the background mesh, was constructed. The computational domain is divided into multiple regions with varying mesh sizes. The smallest grid size is used around the WEC system and the wave zone,

while larger cells are utilized in regions further away from the wave zone and wave-fluid interaction area. The objective is to minimize the total number of grids while maintaining sufficient resolution around the areas of interest. Figure 8 depicts the constructed grid along with the boundary conditions used for the remaining tasks 2-4 of the project.

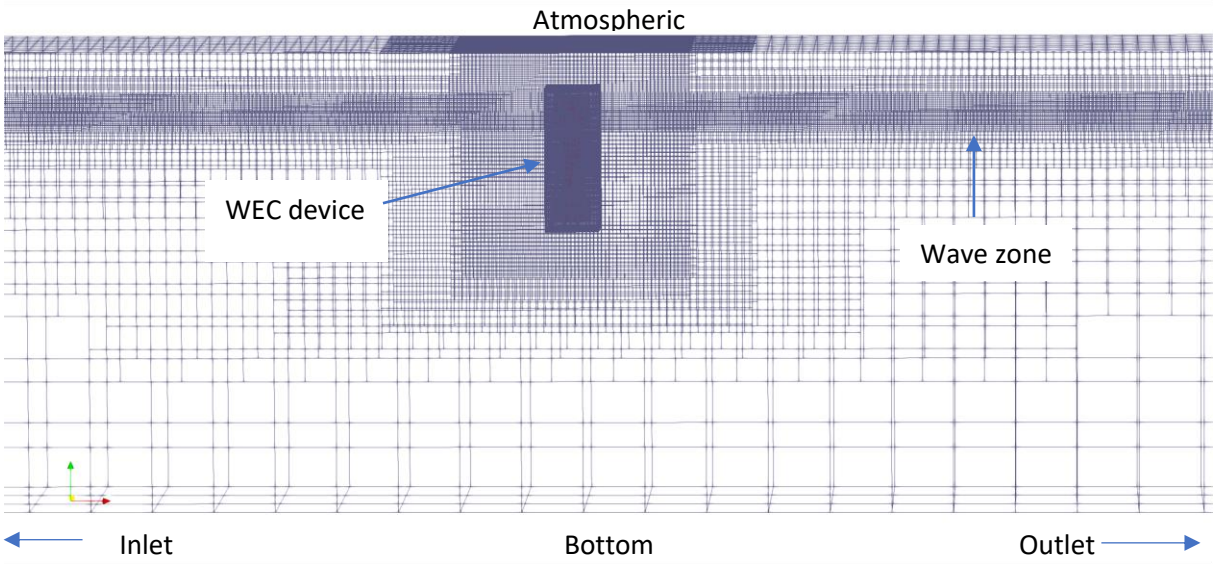

Figure 8: Mesh construction for the numerical simulation. Finest resolution is used for the innermost region where the WEC system is placed, as well as the region at the wave elevation area. Outside these two zones, the grid is coarsening to reduce the computational resources.

7.1.3 Task 2 – Simulation of the fixed device under wave conditions

Four simulation cases of the fixed device subjected to different wave conditions were performed under this Task. The output parameters of this section include the structural loadings in the heave and surge directions, as well as the pressures along the body. Fifty-four pressure probes are placed along the body, with 26 on each side, to measure the surface pressures. The approximate locations of these pressure probes are illustrated in Figure 9.

In the first case, we carried out the simulation of the fixed device subjected to a regular wave condition. The wave period and wave height are derived from the H601 (assumption Rayleigh distribution of the signal) using the dominant wave frequency and an amplified wave height as below. The simulation time (~26 s) is selected such that more than five wave cycles are generated.

$$H = 1.9H_{s(H601)}$$

$$T = T_{p(H601)}$$

The second case is the fixed device subjected to irregular waves using the H601 wave condition. These two cases are performed with the scaled prototype (a scale ratio of 1:28) and with water depth matching the experimental wave tank of 5.8m. A 60-second period (~320 s at full scale) with high wave elevation is selected from the experimental wave signal out of the 3h duration collected from experiments. It is noted that the results in this section are not directly compared to the experimental data due to the lack of tank measurements. They are, however, utilized to evaluate whether the regular wave condition, derived from the maximum wave components and amplified by a factor of 1.9, can yield conservative results compared to simulations using the full irregular wave condition.

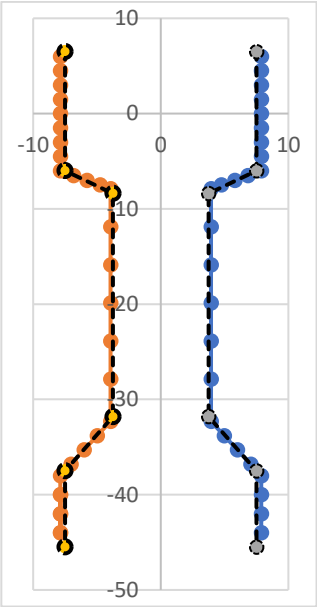

Figure 9: Pressure probe locations on each side of the body. The dimensions shown are meters in full scale.

For these first two cases, maximum pressure outputs at each probe along the body are extracted from the simulations and plotted in Figure 10. The probe numbers are ordered from top to bottom on the WEC with 26 probes on each side. The pressure values from the regular wave condition can be observed to consistently be higher than the irregular wave case. As expected, higher pressures are measured for probes at the WEC's bottom compared to the top surfaces. The results in this section demonstrated that structural loadings subjected to irregular wave conditions could be conservatively estimated employing the regular wave height and a multiplied factor of 1.9. The total loadings in surge and heave directions on the WEC body are presented in Figure 11.

The remaining two cases were conducted with full-scaled model and with the water depth matching the PACWAVE-South condition of 70m. The fixed device are subjected to irregular waves using the D516 and H601 wave conditions. While the pressure data are transferred to IDOM for further processing, the horizontal and vertical forces exerting on the buoy are plotted in Figure 12 for demonstration.

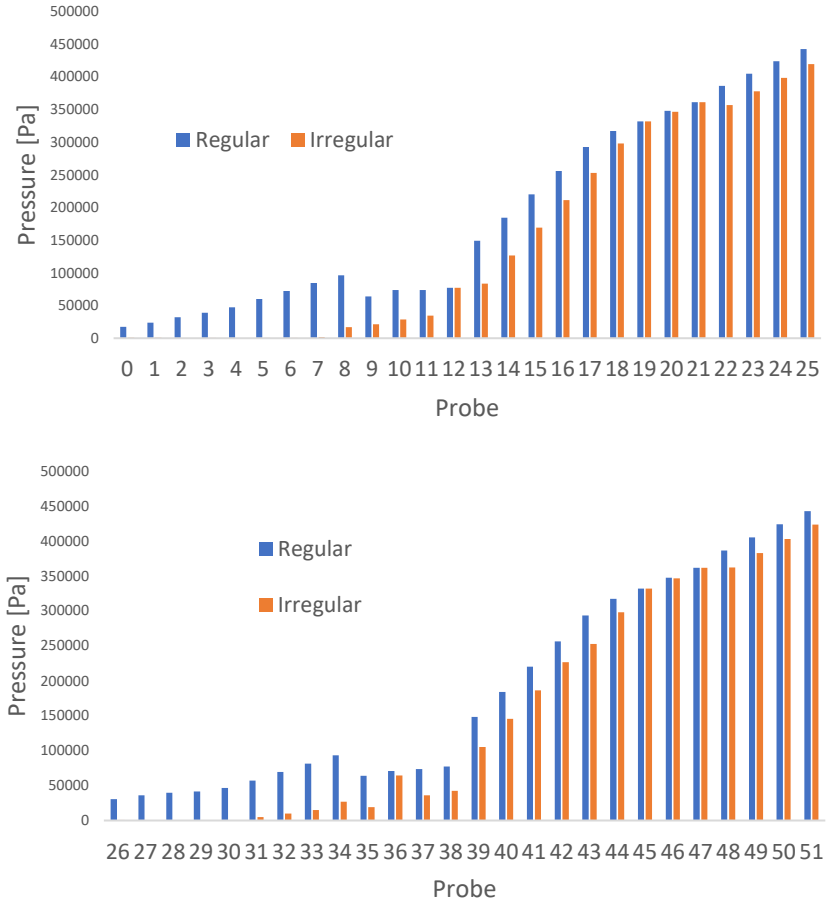

Figure 10: Maximum pressure outputs from the body's surface are presented. 26 probes placed on each side of the body. The maximum pressures are extracted from the hydrodynamic loads as the device subjected to regular and irregular waves.

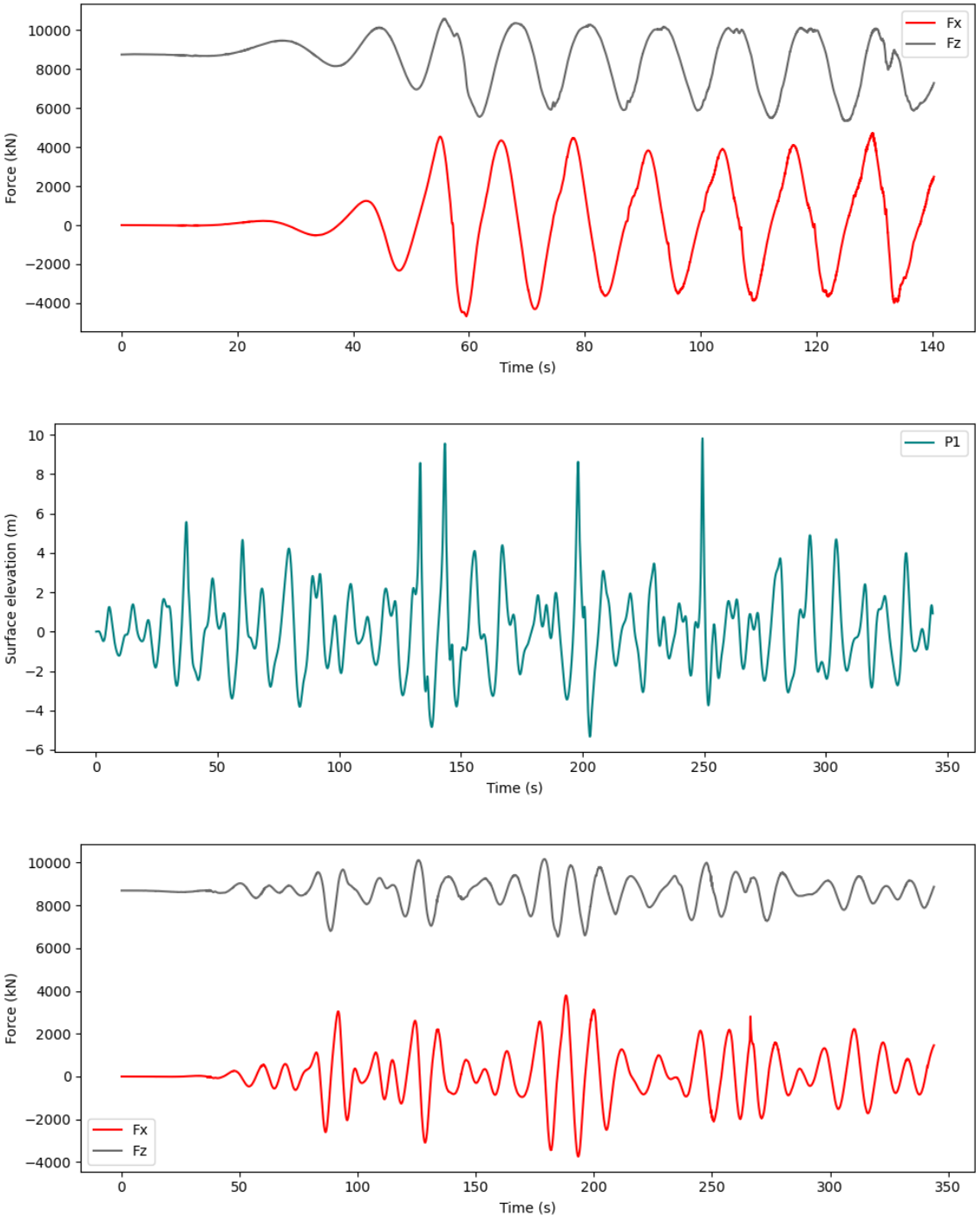

Figure 11: Structural loadings in surge and heave directions for the fixed device case. The WEC system is subjected to both regular (top) and irregular (bottom) wave condition. The regular wave condition are specified as $H = 1.9H_s$ and $T = T_p$. Irregular wave input, which are selected from the range with highest wave elevations, at the inlet of the flume is also presented in the middle plot.

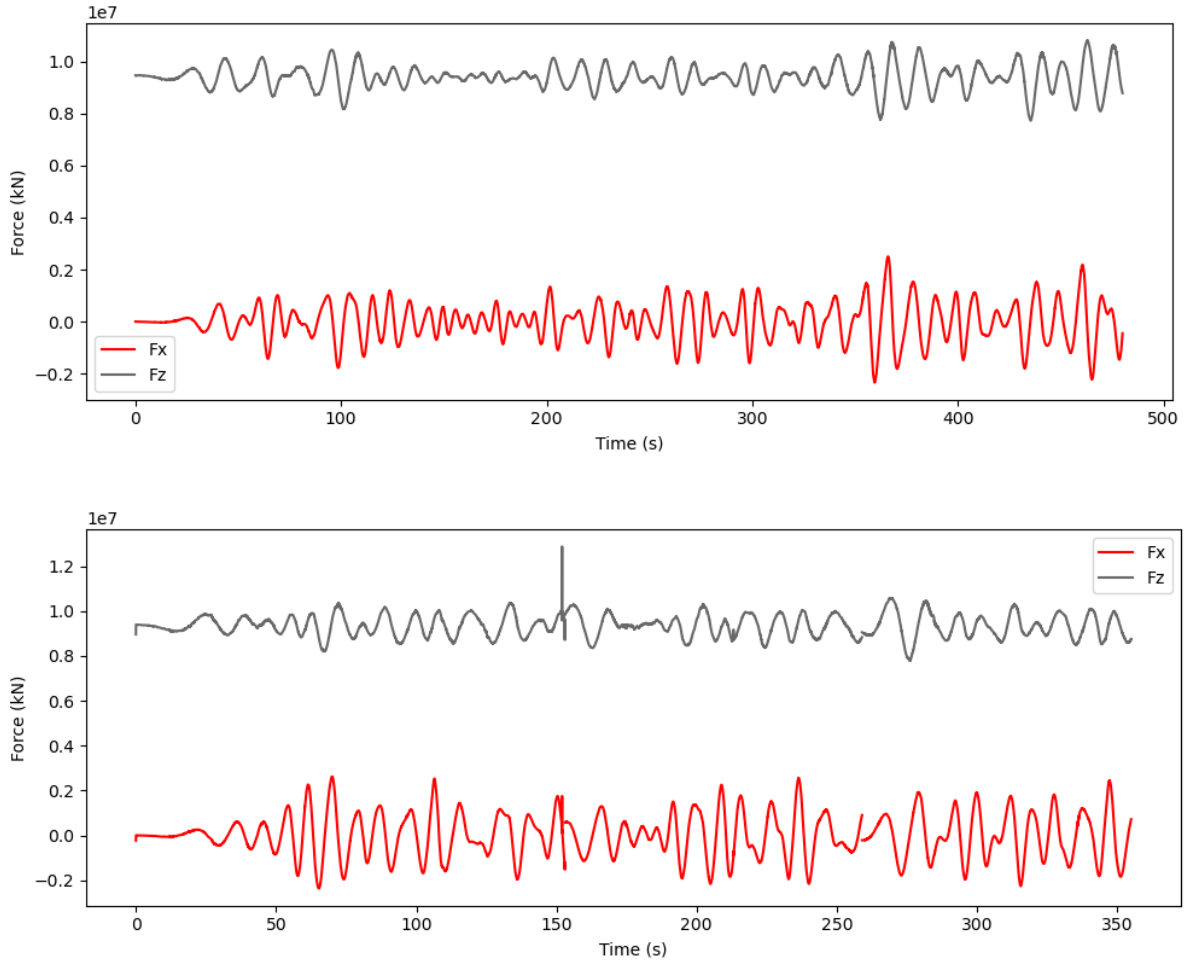

Figure 12: Structural loadings in surge and heave directions for the full-scale fixed device case. The WEC system is subjected to two different irregular wave conditions. Top: D516. Bottom: H601. The irregular wave inputs are selected from the range with highest wave elevations.

7.1.4 Task 3 – Free decay testing of the device and static mooring tests

7.1.4.1 Free decay testing of the device

Free decay tests are performed to quantify the motion of the device when subjected to an initial position offset, either in the heave or pitch degree of freedom. For this study, three free decay tests are carried out, two in heave (with and without the top plate orifice) and one in pitch (without the top plate orifice). The initial offsets were set at 0.125m (scaled at 1:28 ratio) and 3 degrees for heave and pitch, respectively. A mesh convergence study was first performed. The grid sizes are parameterized with the numbers of cells per wave height (using H_s from H601 condition) to keep it consistent with the mesh convergence in the wave only cases. The motion comparisons for different grids are presented in Figure 13.

It is observed that for both heave and pitch free decay of the float without the top orifice, the motion converges relatively well with little differences between the 15 CPH and 20 CPH. For the case of the float with the top orifice, good correlation is also obtained for the first two cycles of the response. Slight deviations are noticed after the second peaks and as the motion amplitude decreases. However, if we compare the calculated damped natural frequency (ω_d) and damping ratio (ζ), differences between the two grid sizes are within 3%. Considering the significant increase in the number of cells needed for the 20 CPH case, we will proceed with the 15 CPH for the remaining simulations.

From the free decay responses, two parameters consisting of the damped natural period (T_d) and the damping coefficient (ζ) are evaluated using a logarithmic decrement method (Inman, 2017) to provide quantitative comparison with the experimental data. While the results are presented in Figure 14 and TABLE 2, the following equations are employed for these calculations.

Damped natural period, T_d:

$$T_d = \frac{1}{n}\sum_{i=1}^{n} T_i \tag{2}$$

Damping coefficient or damping ratio (ζ):

$$\zeta = \frac{\delta}{\sqrt{4\pi^2 + \delta^2}} \tag{3}$$

With

$$\delta = \frac{1}{n}\ln\left(\frac{X_i}{X_{i+n}}\right) \tag{4}$$

Where T_i refers to the time it takes between successive peaks. The logarithmic decrement, δ, represents the rate at which the damped free response amplitude decays. Quantities X_i and X_{i+n} are peaks occurring n cycles apart beginning at the i^{th} oscillation cycle.

From the outputs, it is noted that the heave responses for systems without the top plate orifice closely match the experimental data, showing excellent agreement. The free decay in heave for device with the top plate orifice and the pitch response, however, deviate from the experimental data. TABLE 2 provides a more quantitative comparison between the two datasets, presenting the mean values and associated uncertainties (standard deviation) obtained from the experiments. It is noted that the values are presented as normalized. The amplitudes are normalized against the initial displacement, and the simulated times are normalized with the corresponding experimental damped periods in each case. As evident from Figure 14Figure 13, the heave decay test for the device without the top plate orifice shows great correlation between the numerical predictions and the experimental results. The numerical values fall within the range (mean and uncertainties) recorded from the experimental tests. Conversely, for the heave decay test with the orifice, significant deviations can be observed, particularly in the damping coefficient compared to the experimental data. It is, however, worth noting that the associated uncertainty from experimental measurements for this parameter is substantial, reaching up to 11.73%. Additionally, the heave response exhibits high damping, resulting in only three cycles being recorded in the experiment compared to more than five cycles for the other cases. Since the damping coefficient and natural period are derived with a minimal number of cycles and given the high uncertainty values, these

factors reasonably explain the differences between the two methods. Taking the uncertainty into account, the differences are reduced to within 7.5% and 6.5% for the damping coefficient and natural period, respectively.

On the other hand, the numerically predicted pitch response is noticeably slower and less damped compared to the corresponding experiments. The pitch response is strongly influenced by the position of the center of gravity relative to the water line and the moment of inertia of the buoy. Acceptable measurement errors in these physical quantities can result in significant differences in pitch for models at the testing scale. It has been shown in other studies that even small uncertainties in center of gravity measurements can lead to substantial variations in pitch free decay results. Furthermore, these variations could also be attributed to the viscous effects. The turbulence model and the use of wall functions may underestimate the turbulent viscosity surrounding the body, thereby affecting the damping forces. Radiation damping in pitch is considerably smaller than in heave for this type of OWC, which explains why the viscous damping forces have a greater relative impact on the total damping in pitch compared to heave. This explains the better correlation of the results in heave compared to pitch.

TABLE 2
FREE DECAY RESPONSE (NORMALIZED) COMPARISON

		Experiment	OF	ε (%)
Heave (no orifice)	ζ $(-)$	0.0233 (0.0034)	0.024	3.00 (± 14.59)
	T_d $(-)$	1.000 ($\pm$ 0.22)	1.01	1.00 (0.22)
Heave (with orifice)	ζ $(-)$	0.0895 (0.0105)	0.107	19.55 ($\pm$ 11.73)
	T_d $(-)$	1.000 (± 1.63)	0.917	8.32 (± 1.63)
Pitch (no orifice)	ζ $(-)$	0.0112 (0.0003)	0.012	7.14 (± 0.27)
	T_d $(-)$	1.000 (± 0.08)	1.064	6.41 (± 0.08)

* Values in parentheses are associated with the uncertainties (standard deviations) from the experimental data.
** The damping ratios are normalized against the initial displacement, and the damped periods are normalized with the corresponding experimental values in each case.

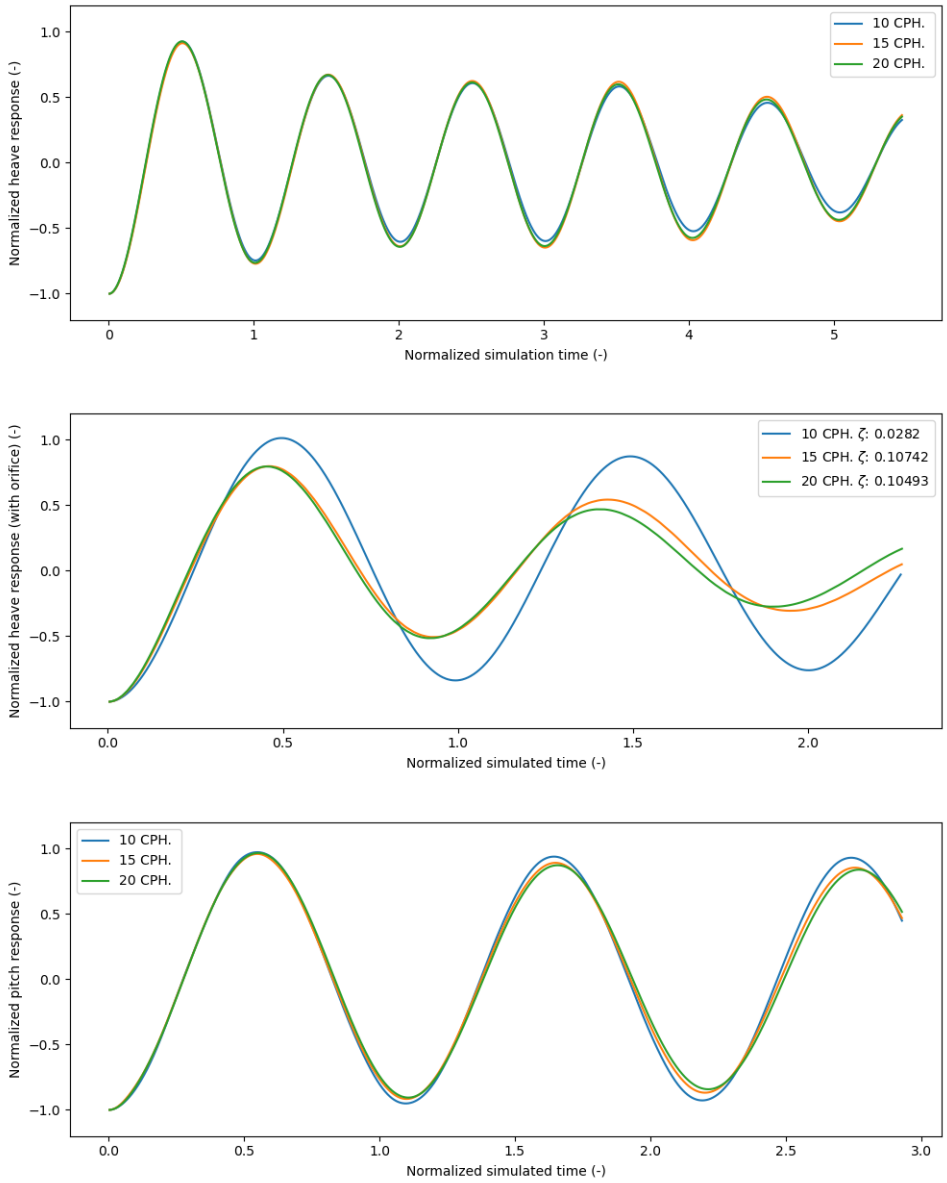

Figure 13: Mesh convergence of free decay tests for a) heave response for system without orifice, b) heave response for system with an orifice, and c) pitch response for system without an orifice. Test grid sizes are from 10, 15, and 20 cells per wave height (based on the H601 wave height case). The amplitudes are normalized against the initial displacement, and the simulated times are normalized with the corresponding experimental damped periods in each case.

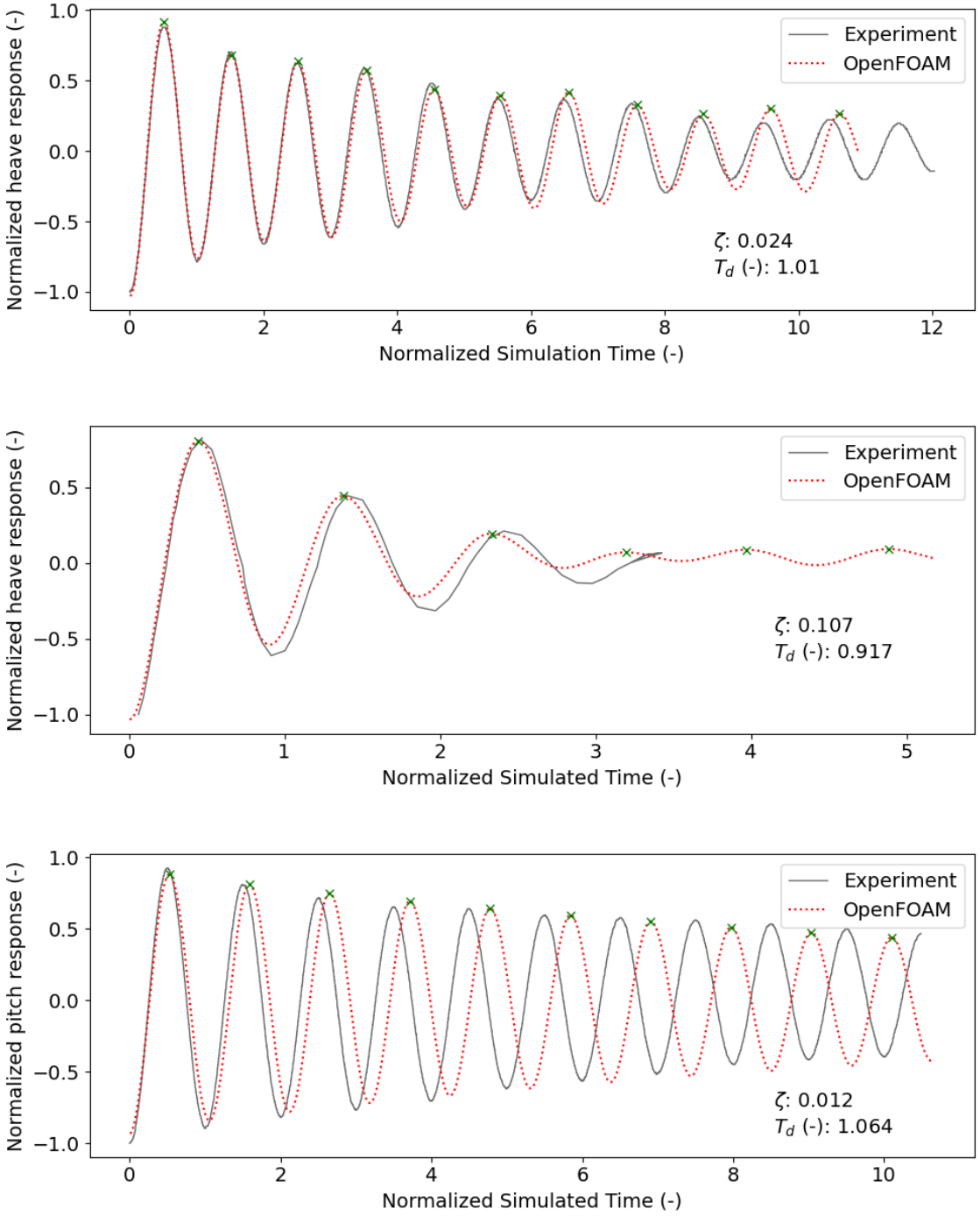

*Figure 14: Free decay tests for a) heave response for system **without orifice**, b) heave response for system **with an orifice**, and c) pitch response for system **without an orifice**. The amplitudes are normalized against the initial displacement, and the simulated times are normalized with the corresponding experimental damped periods in each case.*

7.1.4.2 *Static mooring tests*

The mooring system comprises four primary mooring lines that connect the four floats on the water surface to the seabed. These floats are interconnected by four Celda lines, while another set of four Conex lines links the floats to the WEC device. Figure 15 depicts a visual representation of the overall mooring system.

Before performing the coupled floating simulations, the mooring configuration is benchmarked against experimental static test results. To carry out this section, the WEC body is displaced slowly/quasi-statically in the positive surge direction for 1.14 m (or 32 m full scale). The pulling horizontal forces along with the lines' tensions on the main mooring line 4, the Celda D line, and the Conex 1 line are recorded simultaneously. The entire mooring system in this study is handled by MoorDyn including the dynamics and kinematics of the four floats.

The mooring force outputs from the static test are presented in Figure 16, with corresponding experimental data plotted for comparison. The results indicate a good agreement between the two approaches in terms of mooring forces. Some minor deviations are observed specifically in the surge motion versus total pulling horizontal force. These deviations may be attributed to the uncertainty in the pulling trajectory of the system. In the OpenFOAM model, the pulling trajectory can be precisely controlled in the positive surge direction, whereas slight course deviations might occur during the experiments, leading to the observed differences. Nevertheless, these differences are minimal and do not appear to significantly influence the tensions in the mooring lines.

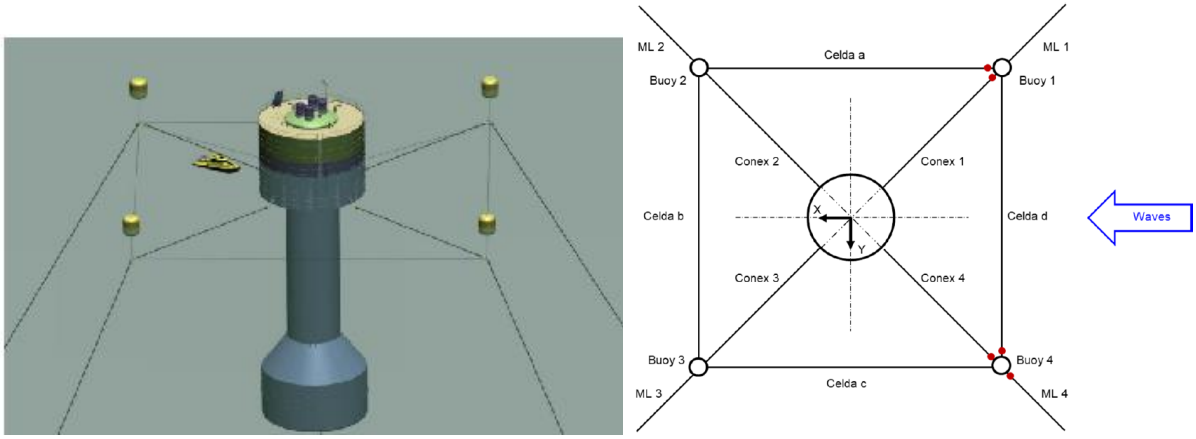

Figure 15: Mooring system diagram for the current system. The mooring system comprises four primary mooring lines that connect the seabed to four floats positioned on the water surface. These floats are interconnected by four Celda lines, while another set of four Conex lines links the floats to the WEC device.

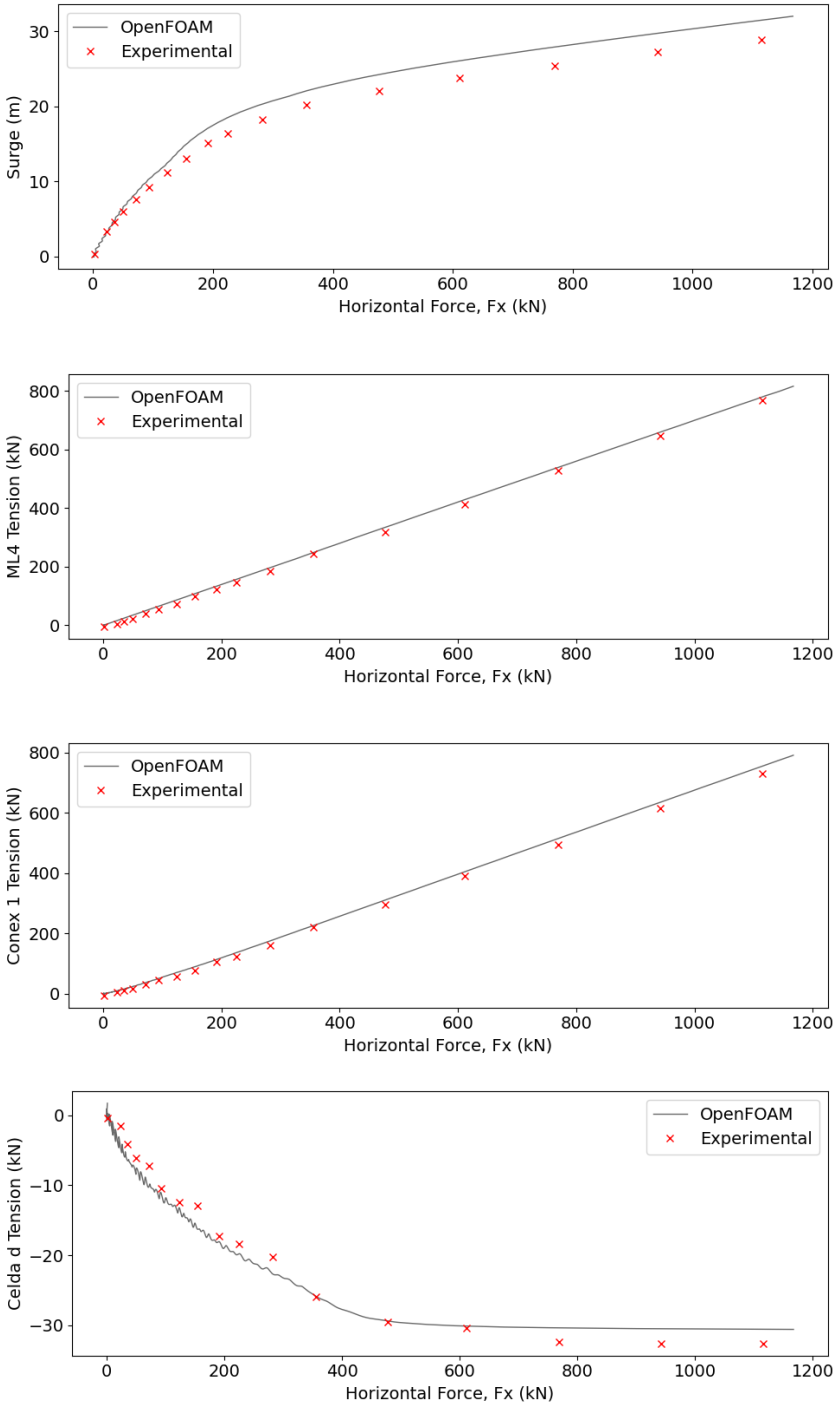

Figure 16: Mooring tension results from quasi-static tests. For this test, the buoy is move quasi-statically in the positive surge direction while the total forces acting on the WEC and the mooring tensions are recorded.

7.1.5 Task 4 – Fully coupled simulation of wave-induced device motion

Four fully coupled simulation of the wave-induced device motion were carried out. While the first two cases were simulated to benchmark the model via comparison with experimental data, the last two cases were conducted to simulate the full-scale device with physical site water depth. Figure 17 below illustrate the simulation outputs of the full MARMOK-OWC device and its realistic mooring system (catenary/chain and polyester ropes).

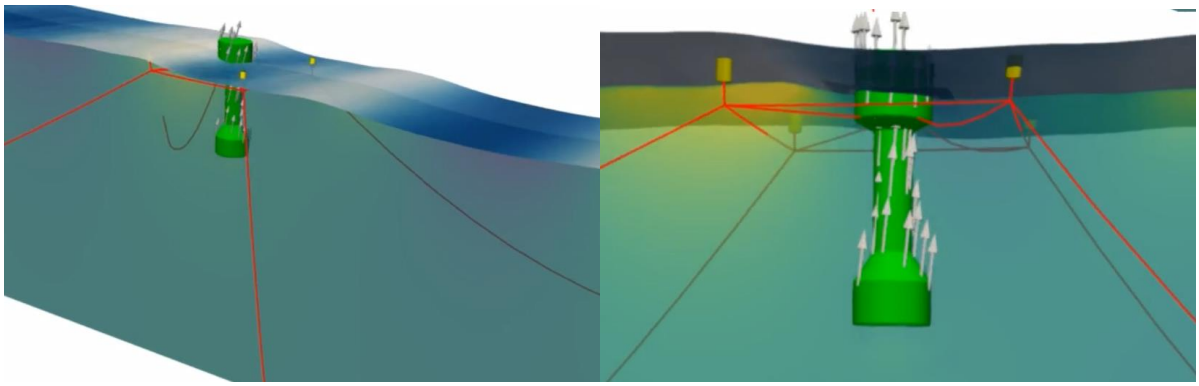

Figure 17: Illustration of the numerical model of the MARMOK-OWC and its mooring system, which consists of chain, ropes, and the connecting floats.

a. D516 wave condition – scaled model:

Figure 18 and Figure 19 display the motion responses of the WEC and the corresponding mooring tensions. In Figure 18, similar to the H601 case, a strong correlation is observed between the heave and pitch motions in both the numerical model and experimental data. For the surge response, the numerical model and experimental data deviates from the start of the simulations. While the WEC's position remains relatively constant in the experiment, it drifts slowly away from the starting position from the time marks of 25s to 100s. After 100s mark, the float is seen to reach its maximum offset position. Disregarding the shift resulting from the drift, the trends in the two curves demonstrate great agreement. The reason for the deviation is currently unknown and will be investigated in future analysis.

Figure 19 presents a comparison of the tensions in the main mooring line 4, and the Conex 1 line. The numerical output exhibits good agreement with the experimental data, excluding the initial few cycles due to the ramping time. Shifts in the magnitude of the simulation lines' tensions compared to the measured data, however, are observed. These shifts can be attributed to the deviation of the WEC's surged position discussed in previous paragraph. The trends of the two datasets, however, correlate well with one another.

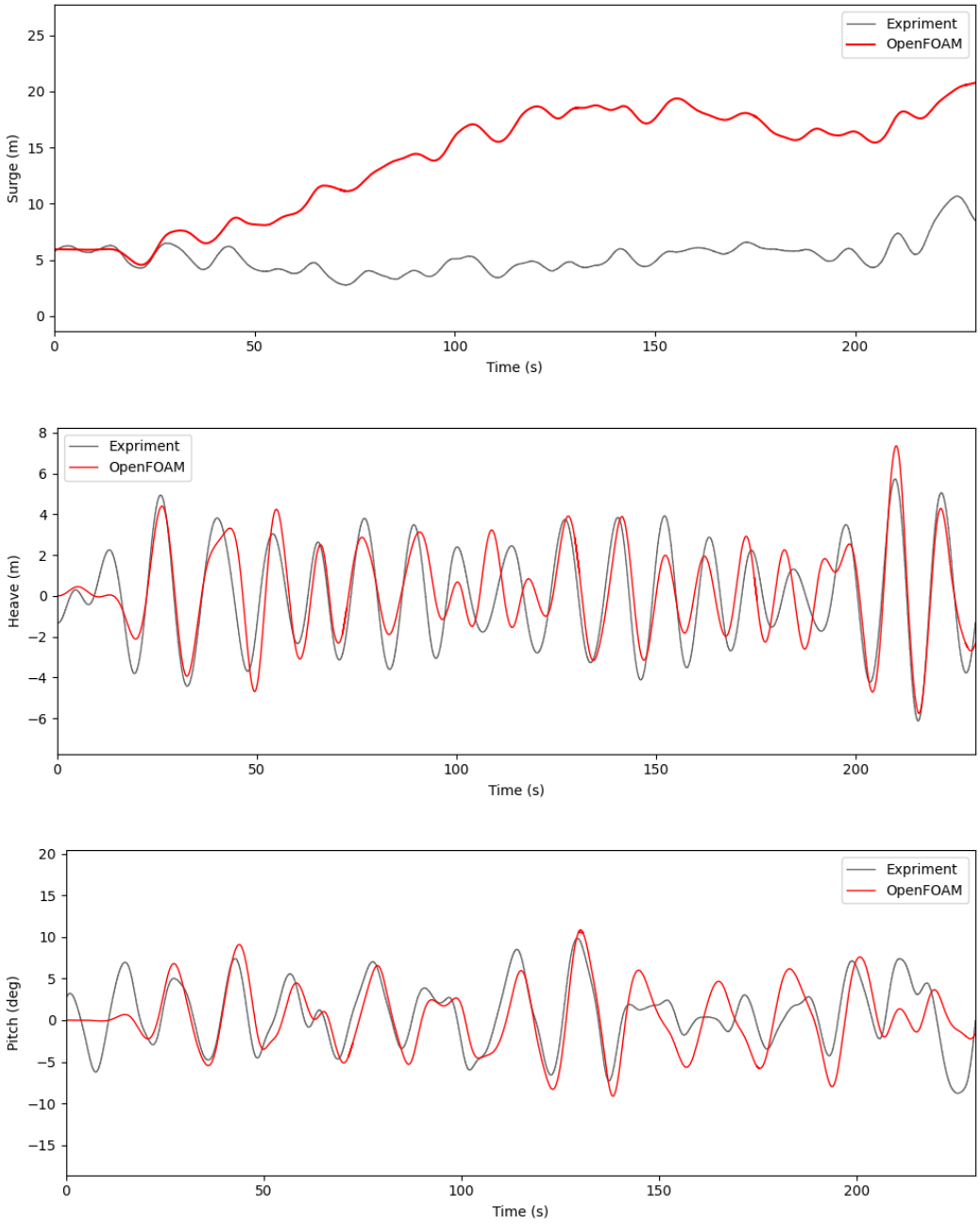

Figure 18: D516 Fully Coupled Simulation of Scaled Model - Comparisons of the WEC's responses in Surge, Heave, and Pitch directions subjected to the first 250s of the irregular wave train between experimental and numerical methods. Heave and pitch results show very good correlation between the two datasets. For the surge response, the numerical model and experimental data deviates from the start of the simulations. While the WEC's position remains relatively constant in the experiment, it drifts slowly away from the starting position from the time marks of 25s to 100s. After 100s mark, the float is seen to reach its maximum offset position.

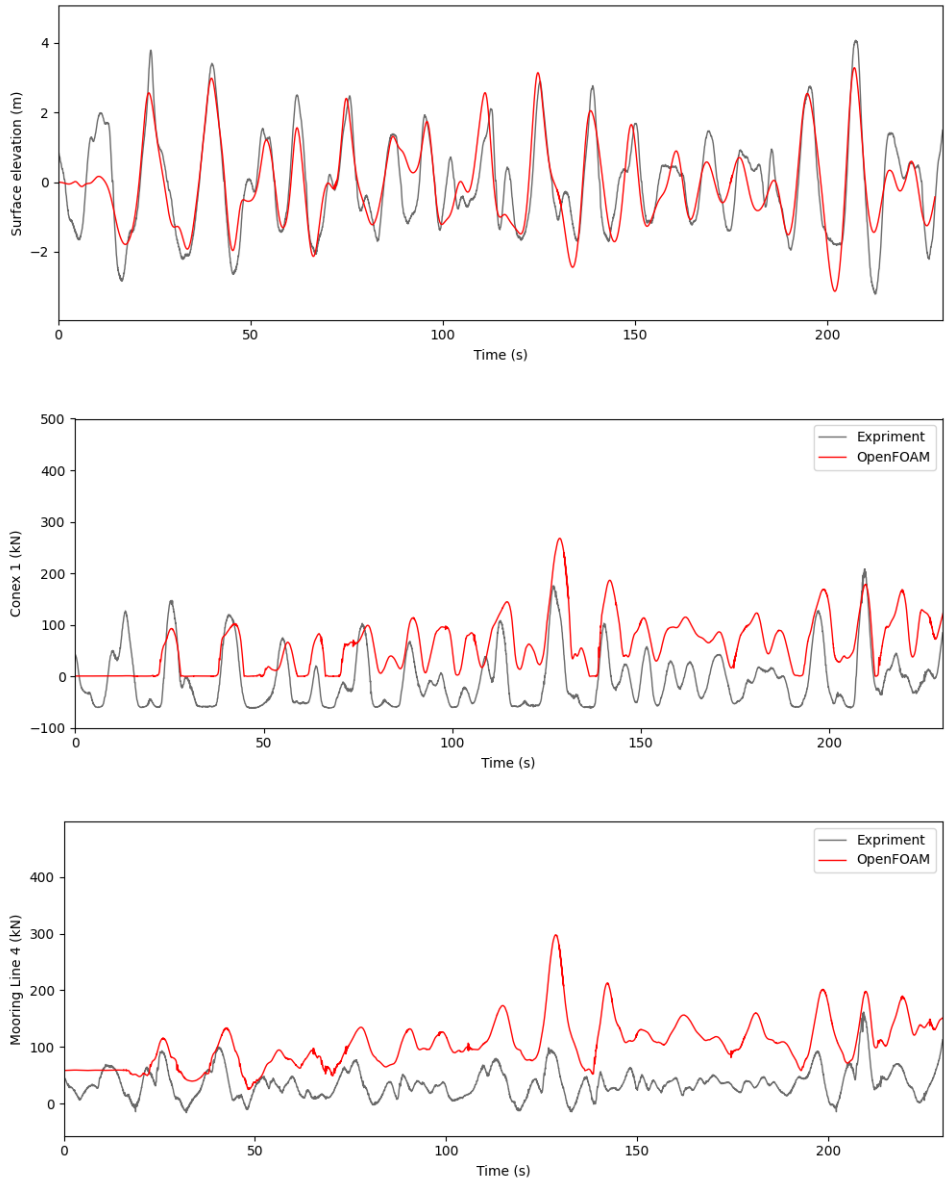

Figure 19: D516 Fully Coupled Simulation of Scaled Model - Comparisons of the mooring tensions in the main mooring line 4, Conex 1, and Celda D when the WEC is subjected to the first 250s of the irregular wave train.

b. H601 wave condition – scaled model:

Figure 20 and Figure 21 display the motion responses of the WEC and the corresponding mooring tensions. In Figure 20, a strong correlation is observed between the heave and pitch motions in both the numerical model and experimental data. For the surge response, the numerical model and experimental data exhibit good agreement for the initial 60 seconds. Deviations, however, become noticeable between 60 and 120

seconds. During this period, while the WEC's position remains relatively constant in the simulation, it moves back towards the starting position in the experiment. Correspondingly, the wave loads appear to be larger in the OF model compared to the laboratory forces. Beyond the 120-second mark, disregarding the shift resulting from the previous period, the trends in the two curves demonstrate great agreement. The reason for the deviation between 60 and 120 seconds is currently unknown and will be investigated in future analysis.

Figure 21 presents a comparison of the tensions in the main mooring line 4, and the Conex 1 line. The numerical output of Conex 1 exhibits good agreement with the experimental data, excluding the initial few cycles due to the ramping time. Regarding mooring line 4, the trend of the tension curve and its upper bound envelope closely correlate with the laboratory data. Starting from approximately 70 seconds, however, a shift in the magnitude of the simulation line's tensions compared to the measured data is observed. This shift can be attributed to the deviation of the WEC's surge position between 60 and 120 seconds. Future study should explore these differences further.

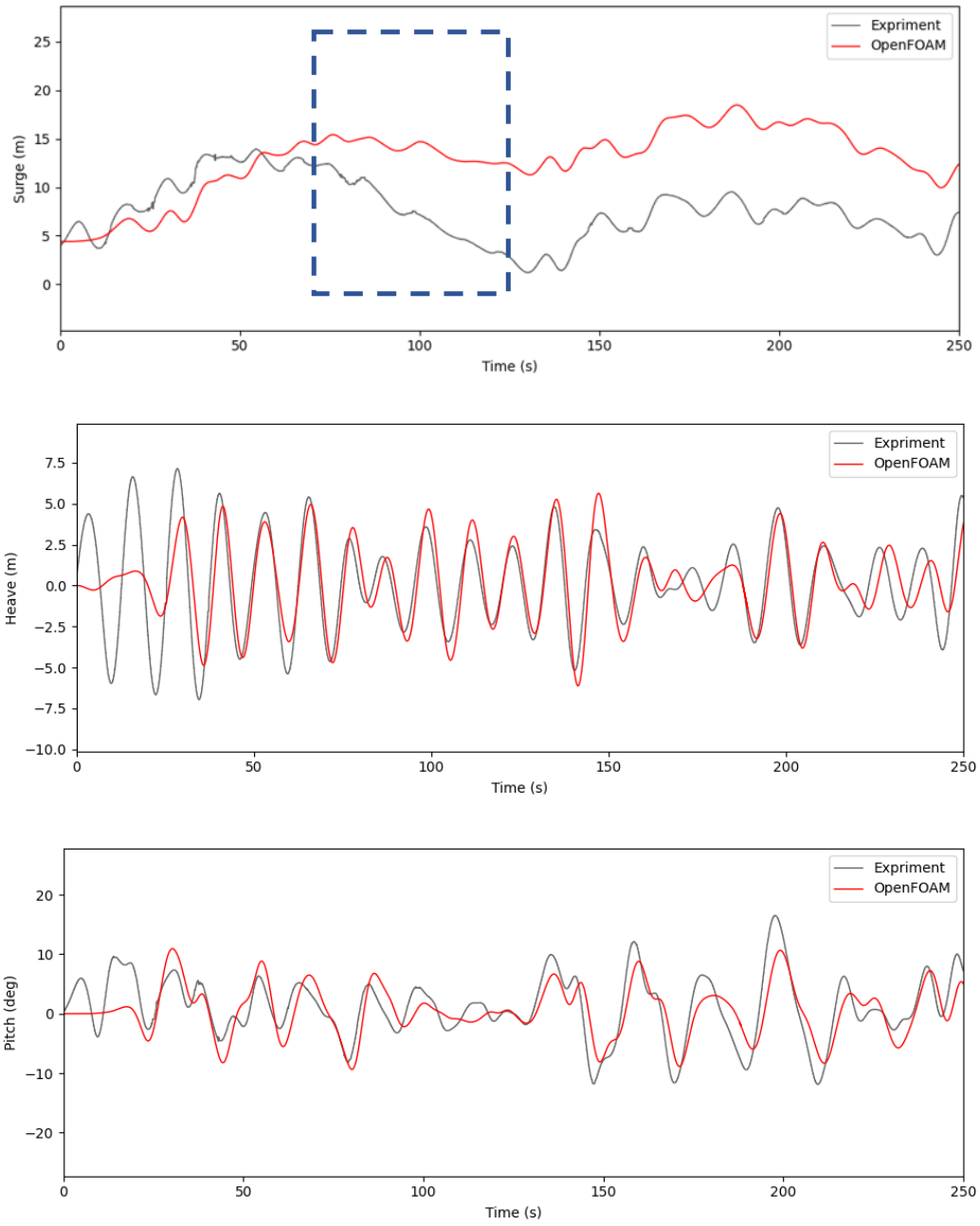

Figure 20: H601 Fully Coupled Simulation of Scaled Model - Comparisons of the WEC's responses in Surge, Heave, and Pitch directions subjected to the first 250s of the irregular wave train between experimental and numerical methods. Heave and pitch results show very good correlation between the two datasets. Surge responses are also compared well except for the time marks from 60-120s (denoted by the dash box).

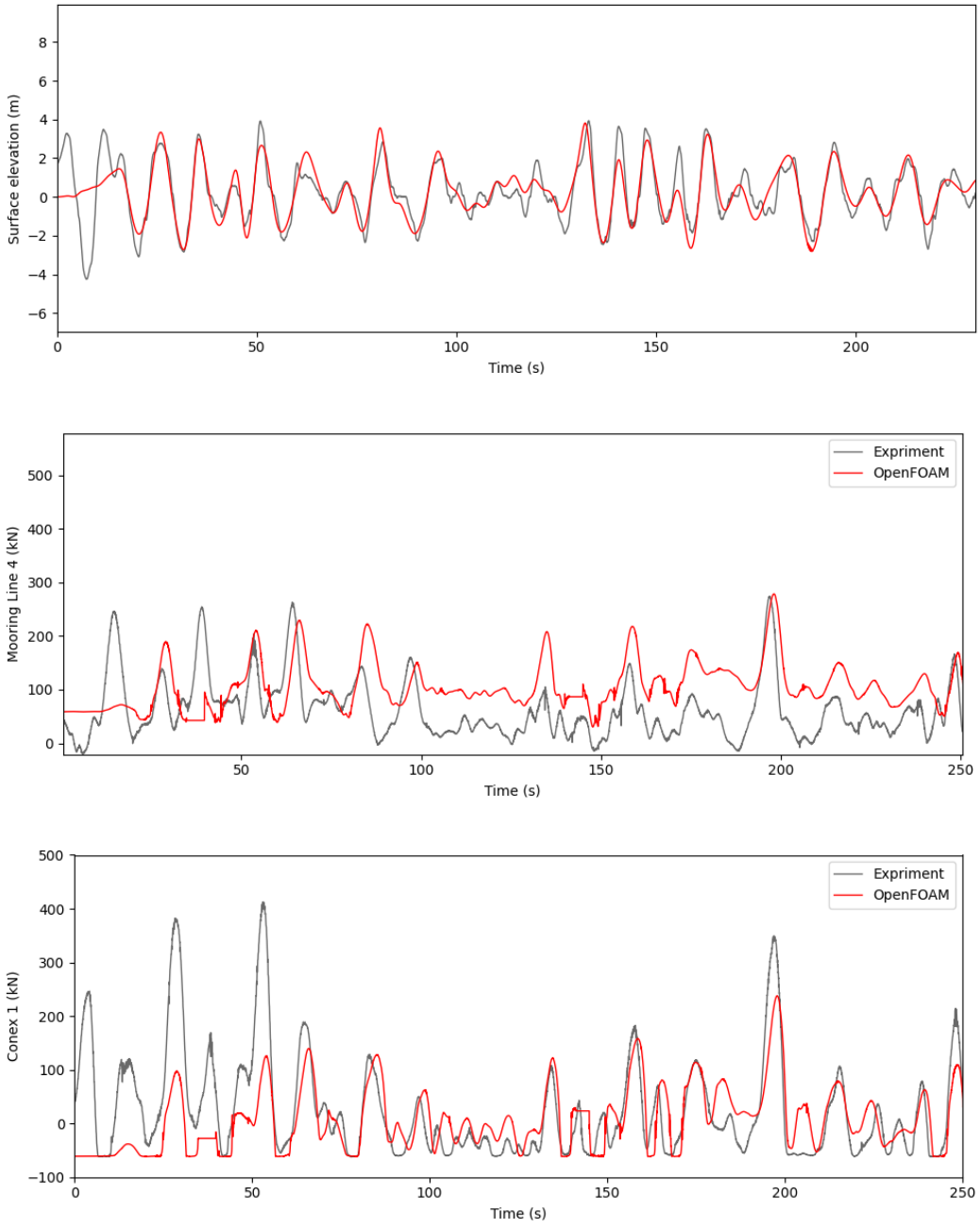

Figure 21: H601 Fully Coupled Simulation of Scaled Model - Comparisons of the mooring tensions in the main mooring line 4, Conex 1, and Celda D when the WEC is subjected to the first 250s of the irregular wave train.

c. D516 wave condition – full scale and different mooring configuration:

A period of 350 seconds (full scale at a 1:28 ratio) is selected from the time series of wave elevation shown in Figure 6: for the simulation in this section, which aims to study the fully-coupled system under extreme wave conditions. Note that the wave data in Figure 6: is scaled so that 350 seconds at full scale is equivalent to about 60 seconds of wave signal at full size. The wave signal is selected from the 300-second mark in Figure 6, representing one of the highest wave trains in the signal. While the parameters of interest, including body surface pressure, body motions, upstream wave elevations, and mooring tensions, are exported and transferred to IDOM, Figure 22 illustrate the time series of those datasets.

Figure 22: D516 Fully Coupled Simulation of Full Size Model with Different Mooring System- Illustrations of the body motion along with the mooring tensions when the WEC is subjected to a period of 350 s of high wave elevations.

d. H601 wave condition – full scale and different mooring configuration:

Similar to the previous case, a period of 350 seconds (full scale at a 1:28 ratio) is selected from the time series of wave elevation, representing one of the highest wave trains in the signal. The simulation in this case incurred instability around 170 seconds into the process (Figure 23). The wave conditions in this case exhibit higher nonlinearity effects compared to the previous case, likely leading to greater fluctuations in the system's motions and the resulting instability. After 100 seconds into the simulation, significant heave and pitch were noticed while the system was still surging due to wave-induced motion. This might have led to the high increase in the lines' tensions as demonstrated in the figure below. Due to the project's time constraints, we were unable to resolve these issues within the given timeframe. It is noted that while this case is incomplete, the Task 4 objective is considered met with the production of the three cases

Figure 23: H601 Fully Coupled Simulation of Full Size Model with Different Mooring System- Illustrations of the body motion along with the mooring tensions when the WEC is subjected to a period of 170 s of high wave elevations.

described above. This additional case was attempted as time permitted. The parameters of interest, including body surface pressure, body motions, upstream wave elevations, and mooring tensions for the 170-second period were exported and transferred to IDOM. Figure 23 illustrates the time series of these datasets.

e. Other data of interest:

Surface pressures in these cases are exported and shared with IDOM for further offline analysis. Samples of the pressure dataset are presented in Figure 24 below:

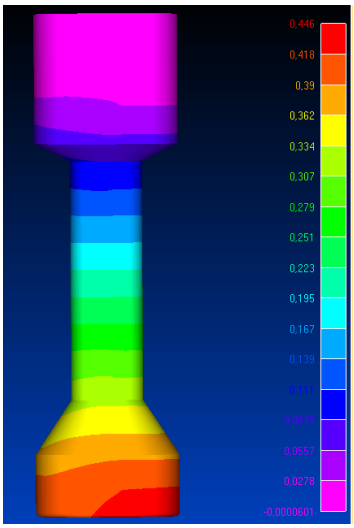

Figure 24: Pressure mapping for FEA analysis (post-study completed by IDOM).

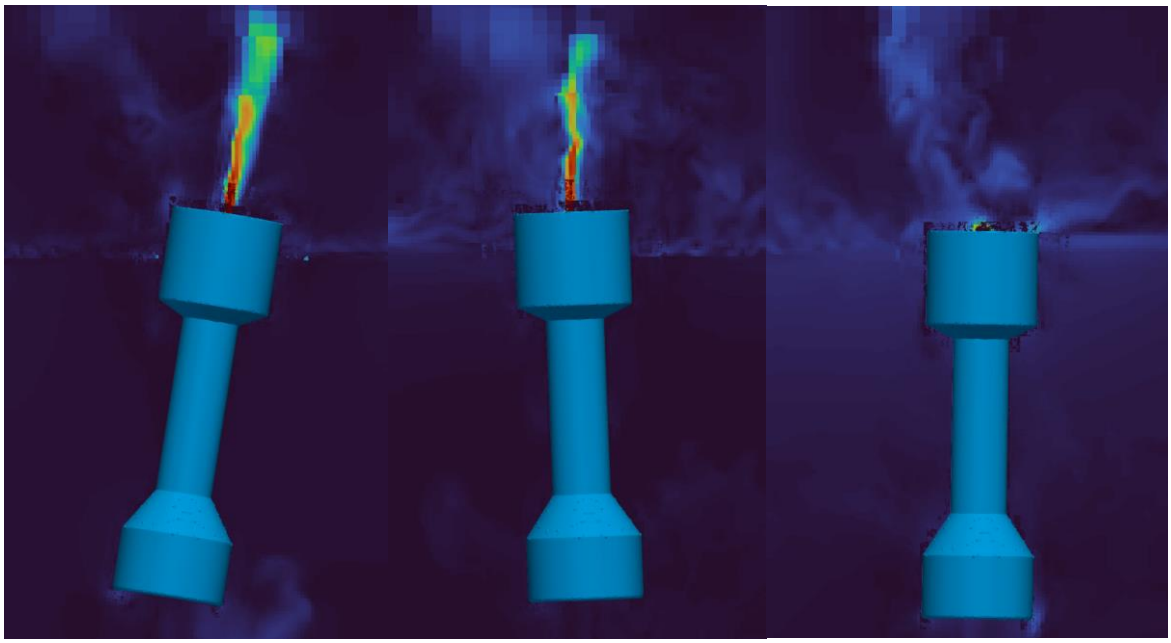

Figure 25: Sub-figures illustrate the velocities exiting the orifice at different time periods.

Velocities around the orifice are also extracted and shared with IDOM. Figure 25 depicts the flow velocities exiting the orifice at different time periods, while Figure 26 presents the time series of velocity components and magnitudes for the D516 and H601 cases with the new mooring design.

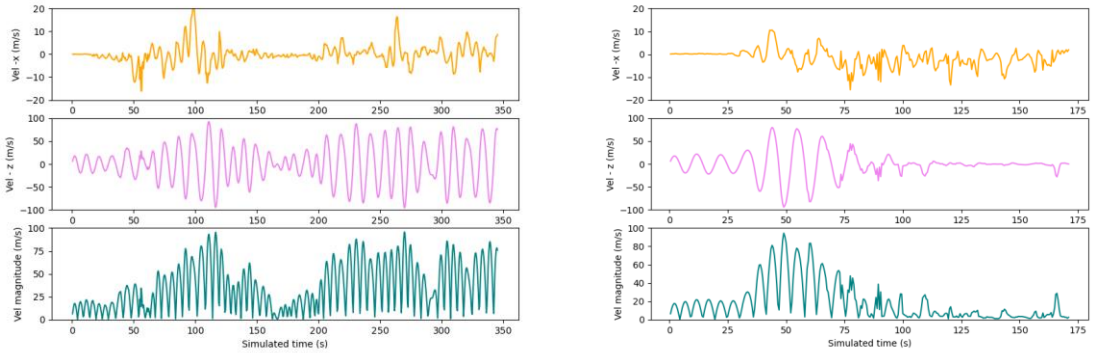

Figure 26: Left – Time series of velocity components and magnitudes for the D516 case (new mooring design). Right: Time series of velocity components and magnitudes for the H601 case (new mooring design).

7.2. Lesson Learned and Teat Plan Deviation

7.1.6 Lessons Learned

Some lesson learned during this project are that it is easy to underestimate the difficulties of implementing numerical models of wave energy devices. The timescales required for running models, even using the multi-processor system at NTESS/SNL, are significant given the resolution required in the model and the large number of grid points required in the simulation domain. Sandia were able to accommodate this expanded time schedule but it is an important feature to consider in estimating the effort required in future projects.

Simulations in this project were carried out using leading-edge simulation technologies. As part of the project, a methodology was developed to recreate the wave signal (time series matching each instantaneous wave elevation) obtained from laboratory tests, improving comparisons between experimental and numerical datasets. Additionally, the project integrated the open-source mooring toolbox MoorDyn into OpenFOAM to simulate realistic mooring systems, as opposed to the typically utilized simplified linear spring and damper model. This integration provides a tool for simulating realistic mooring systems for wave energy converters using entirely open-source programs.

Additionally, it is noted that due to time constraints, the mesh selection and different resolutions, especially in the region away from the WEC system, could be still be optimized further to reduce simulation times without compromising accuracy of results in future study.

7.1.7 Test Plan Deviation

The performance deviated from the test plan only in the timeline. Administrative complications with the Cooperative Research and Development Agreement (CRADA), HPC resource availability, high demand for computational resources to develop and simulate high-fidelity 3D numerical models, and personal time off events all had an impact on the duration of the project.

8 Conclusions and Recommendations

The primary outcome from this project is the production of numerical simulations of the behavior of the IDOM's MARMOK-OWC wave energy converter along with its mooring system subjected to extreme wave conditions. The data derived from the simulations will be used by IDOM to validate the structural integrity (surface loading/pressure) during extreme events. The results will also be employed to inform future iterations of the MARMOK-OWC device. This is expected to enhance the performance of the system and lead to reduced LCOE.

In Task 1, three different extreme sea state time series were successfully recreated in numerical simulations using wave elevations provided by IDOM from tank test data. In Task 2, the MARMOK-OWC system was simulated under two of these irregular sea states (one sea state was not simulated due to time constraints). From the simulations, wave pressures on the hull structure were extracted and provided to IDOM for further study of structural loadings. Task 3 included numerical simulations of free-decay tests, which showed good comparisons with experimental data. In Task 4, we successfully integrated OpenFOAM and MoorDyn to realistically model the physical mooring system, consisting of chains, poly ropes, and connecting floats. We also conducted four fully coupled simulations for two different hull scales and two mooring configurations. While three simulations were completed successfully, one simulation resulted in instability when the device was subjected to the highest nonlinear wave signal. Due to project time constraints, further investigation was not feasible, but this issue will be of interest for future study and funding.

Some lesson learned during this project are that it is easy to underestimate the difficulties of implementing numerical models of wave energy devices. The timescales required for running models, even using the multi-processor system at NTESS/SNL, are significant given the resolution required in the model and the large number of grid points required in the simulation domain. Sandia were able to accommodate this expanded time schedule but it is an important feature to consider in estimating the effort required in future projects.

9 References

[1] Inman, D. J. (2017). *Vibration with control*. John Wiley & Sons.

[2] Holthuijsen, L. H. (2010). *Waves in oceanic and coastal waters*. Cambridge university press.

10 ACKNOWLEDGEMENTS

Sandia National Laboratories is a multimission laboratory managed and operated by National Technology & Engineering Solutions of Sandia, LLC, a wholly owned subsidiary of Honeywell International Inc., for the U.S. Department of Energy's National Nuclear Security Administration under contract DE-NA0003525.

Experimental data used for the numerical model validation was obtained through funding provided by the U.S. Department of Energy Office of Energy Efficiency and Renewable Energy Water Power Technologies Office under Award Number DE-EE0008952.

11 APPENDIX

N/A.